Research Square

Preprints are preliminary reports that have not undergone peer review.
They should not be considered conclusive, used to inform clinical practice,
or referenced by the media as validated information.

Insights into combined adhesion-mediated and acquired resistance of ovarian cancer cells to PARP inhibitors highlight ERK as a target for sensitization

Leon Bade
University of Bonn
Lucas Kracht
University of Bonn
Helena Skalski
University of Bonn
Stéphane Brézillon
Université de Reims Champagne-Ardenne
Valérie Untereiner
Université de Reims Champagne-Ardenne
Ganesh D Sockalingum
Université de Reims Champagne-Ardenne
Jindrich Cinatl
Deutsche Kinderkrebsstiftung
Martin Michaelis
University of Kent
Philipp König
philippkoenig@uni-bonn.de

University of Bonn
Gerd Bendas
University of Bonn

Research Article

Keywords: Ovarian Cancer, Chemoresistance, PARP-Inhibitor, Collagen Type I, CAM-DR, DNA repair

Posted Date: November 13th, 2026

DOI: https://doi.org/10.21203/rs.3.rs-11035673/v1

License: This work is licensed under a Creative Commons Attribution 4.0 International License.
Read Full License

Additional Declarations: No competing interests reported.

Abstract

Purpose

Cell adhesion-mediated drug resistance (CAM-DR) is a major reason for therapy failure in oncology. Its relevance for treating acquired PARP inhibitor (PARPi)-resistant ovarian cancer cells has barely been evaluated so far.

Methods

PARPi-resistant W1NR cells were established by treatment of the ovarian cancer cell line W1 with incrementally increasing niraparib concentrations. Cell viability was measured by MTT and annexin V/PI apoptosis assays. Flow cytometry was applied for cell cycle analysis and Western blots for detecting protein levels. Changes in cell surface composition were evaluated via FTIR spectroscopy.

Results

Cultivation on collagen type 1 (COL1) had complex effects on cell sensitivity to PARPi in a series of ovarian cancer cells, which were not related to cell adhesion proteins integrin β1 and DDR1. COL1 enhanced DNA repair protein expression in W1 and cisplatin-resistant W1CR cells, differing from W1NR cell behavior. Contrary to PARPi-naïve cells, COL1 did not further enhance PARPi resistance in W1NR cells. While inhibition of ATR or ATM sensitized W1NR cells to the PARPi niraparib and olaparib in absence of COL1, COL1-cultivation negated the effectiveness of this combination treatment. However, ERK was identified as a promising target to overcome acquired PARPi resistance, independent of COL1-mediated CAM-DR.

Conclusion

Our findings address for the first time the phenomenon of COL1-mediated CAM-DR in ovarian cancer with acquired PARPi resistance. Although COL1 impairs sensitization to PARPi by targeting the DNA repair kinases ATR and ATM, inhibition of ERK1/2 appears as key-strategy for overcoming combined CAM-DR and acquired PARPi resistance.

1 Introduction

Ovarian cancer is one of the deadliest gynecological malignancies [1, 2]. Major reason for the poor treatment outcomes include that ovarian cancer is often diagnosed at a late advanced stage and that the development of chemoresistance is common [3]. Historically, 5-year overall survival rates typically ranged from 10 % to 40 for adanced disease [1, 2]. In the meantime, paclitaxel and platinum-based first line therapies are often complemented with bevacizumab and/or poly adenosine diphosphate ribose

polymerase inhibitors (PARPi) [4]. Notably, the addition of PARPi has been reported to increase the overall 5-year survival rate of patients with advanced-stage ovarian cancer to approximately 70 % [5, 6].

Members of the PARP family, particularly PARP1 [7, 8], are involved in the DNA damage response, including the repair of single-strand breaks (SSBR) and the restart of stalled replication forks [9]. PARP enzymes detect DNA damage and generate poly adenosine diphosphate ribose (PAR) chains (PARylation) that are critical in initiating DNA repair. PARP inhibitors induce both a dysfunction in PARP-dependent DNA repair and the formation of cytotoxic PARP1-PARPi-DNA complexes (PARP trapping) [10, 11]. If PARP is inhibited, cells depend on DNA repair by homologous recombination (HR) repair, which is commonly deficient in ovarian cancer cells, rendering them particularly sensitive to PARP inhibitors [12, 13]. Resistance to PARPi is frequently associated with restoration of HR or upregulation of other pathways of the DNA damage response [14, 15]. However, the efficacy of PARPi is limited by acquired resistance formation[16] due to molecular mechanisms that are only partly understood.

The tumor microenvironment, especially the extracellular matrix (ECM) can contribute to drug resistance, a phenomenon referred to as ‘cell adhesion-mediated drug resistance‘ (CAM-DR) [17]. In CAM-DR, the binding of cancer cell surface receptors to ECM triggers multiple oncogenic signaling and promotes resistance to a range of different anti-cancer drugs. Recent studies have shown that the presence of collagen, an ECM constituent, reduces the sensitivity of ovarian cancer cells to PARPi [18, 19], but the underlying mechanisms remain elusive.

Here, we investigated the impact of collagen type 1 (COL1) on the PARPi sensitivity of sensitive and drug-resistant ovarian cancer cells, including PARPi-resistant cell lines. COL1 enhanced DNA repair in all models, albeit by varying mechanisms. We identified ERK as a promising target to overcome combined acquired and CAM-DR PARPi resistance in ovarian cancer cells.

2 Methods

2.1 Cell culture

A2780 and cisplatin-resistant A2780cis cells were received from ECACC, UK (No. 93112519; No.93112517-A2780cis). W1 cells and cisplatin-resistant W1CR cells, first described in [20] were kindly provided by Dr. R. Januchowski (Zielona Gora, Poland). EFO21 cells were obtained from DSMZ (Braunschweig, Germany). Kuramochi cells were obtained from JRCB (Osaka, Japan), whereas its cisplatin-resistant subtype, Kuramochi’CDDP^{2000} was derived from ‘The Resistant Cancer Cell Line (RCCL) collection’ [21]. To maintain the cisplatin-resistance in the respective sublines, cells were regularly treated with 3,000 ng/ml cisplatin (Sigma-Aldrich GmbH, Steinheim, Germany). To avoid cisplatin-induced adulteration, the first passage of the cells following to this selection was not used in experiments. W1 and W1CR cells, in which integrin β1 was depleted using a lentiviral vector, were used as described [19]. All cell lines were cultivated in RPMI 1640 medium (Gibco cell culture solutions, Life Technologies Ltd., Paisley, UK) supplemented with 10% fetal calf serum (FCS) (PAN Biotech GmbH), 100

IU/ml penicillin, and 100 µg/ml streptomycin at 37°C and 5% CO_2. For experiments including collagen matrices, microplates or cell culture flasks were coated with 10 µg/cm^2 COL1 from rat tail (Corning®, Bredford, PA, USA) according to the manufacturer`s protocol. Cultures were monthly tested for the absence of mycoplasma contamination.

2.2 Establishment of niraparib-resistant subline W1NR

Niraparib-resistant W1NR cells were generated by pulse exposure of W1 cells with incrementally increasing doses of niraparib (Hölzel Diagnostika Handels GmbH, Cologne, Germany), reaching a final concentration of 3.2 µM. W1 cells were treated over three passages with the same niraparib dose, each followed by a recovery passage. After three cycles, the dosage was doubled. To preserve niraparib resistance, a maintenance treatment with 3 µM niraparib was applied every second week.

2.3 Cell adhesion assay

After incubating COL1-coated and untreated 96- well microplates (Sarstedt AG & Co, Nümbrecht, Germany) with a 1% solution of bovine serum albumin (BSA) (BIOMOL GmbH, Hamburg, Germany), W1, W1CR, A2780, and A2780cis cells were seeded at a density of 10,000 cells/well and incubated for 24 h. Following the incubation period, cells were washed twice with DPBS, fixed with a 4% paraformaldehyde solution (PFA), stained with a 0.1% methylene blue solution (both from Sigma-Aldrich GmbH), and washed another five times. Absorption was measured at 620 nm using a plate reader (Thermomultiscan EX, Thermo, Schwerte, Germany) after methylene blue was eluted from the cells via 0.1 M hydrochloric acid. Background absorption at 405 nm was subtracted, and the results were normalized to untreated W1 cells.

2.4 Fourier-transform Infrared (FTIR) cellular imaging

To analyze changes in the surface compositions of W1, W1CR, and A2780 cells, they were studied by FTIR imaging with respect to cell surface polysaccharides signatures as previously described [22]. IR-transparent calcium fluoride (CaF_2) windows (Crystran Ltd., Poole, UK) were pre-treated with absolute ethanol for 30 minutes, and coated with COL1 or left uncoated. 30,000 cells were seeded onto the CaF_2 substrates and incubated overnight. They were analyzed using a Spotlight 400 microscope coupled to a Spectrum One spectrometer (Perkin Elmer, Villebon-sur-Yvette, France). Single cells were imaged at 6.25 µm/pixel, spectral resolution of 4 cm^{-1}, and 256 accumulations. Each spectrum is an average of all pixels of an image. For each experiment, about 10–15 single cells were imaged.

2.5 Chemometrics analysis of FTIR spectral data

All cell spectra were baseline-corrected, reduced to the 1400 – 900 cm^{-1} spectral window, doubly derived, normalized, and analyzed by Principal Component Analysis (PCA). Second derivative spectra were used to minimize the baseline influence and resolve overlapping bands. PCA results were shown as 2D-plots of the scores of main principal components (PCs). Corresponding loading plots highlighted the bands determining the separation along each PC. By examining the loadings as spectral lines, chemical

information can be extracted concerning the delineation of the cell data. Since second derivatives were used for calculations, the observed maxima represent the spectra located on the negative side of the corresponding PC, whereas minima highlight bands present in the spectra at the positive side of the PC (scores plot).

2.6 Cell viability assay

To determine cell sensitivity to niraparib and olaparib treatment (both from Hölzel Diagnostika Handels GmbH), either alone or in combination with distinct inhibitors, a MTT (3-(4,5-dimethylthiazol-2-yl)-2,5-diphenyltetrazolium bromide) (BioChemica, Applichem GmbH, Darmstadt, Germany) cell viability assay was performed [18]. Cisplatin was applied as a cytotoxic control. To identify potential targets to sensitize the respective cells to PARPi, cells were pretreated with inhibitors against DDR1/2 (7rh), JNK1/2/3 (tanzisertib), p38 MAPK (adezmapimod), ERK1/2 (SCH772984), ALK/c-Met (crizotinib), pan-PI3K/m-TOR (dactolisib), WNT (pyrivinium), FAK (FAK-IN-14) ATR (elimusertib), and ATM (AZD1390) (all purchased from Hölzel Diagnostika Handels GmbH) for 72 h at sub-toxic concentrations.

All investigated cell lines were transferred in triplicate in 96-well plates (Sarstedt AG & Co). W1, W1CR, W1NR, A2780, and A2780cis cells were seeded at a density of 10,000 cells/well, while EFO21, Kuramochi, and Kuramochi^{r}CDDP^{2000} cells were cultivated at a density of 5,000 cells/well. After an incubation period of 24 h, cells were pre-treated with the respective inhibitor or a control solution. If the inhibitor was dissolved in DMSO (Fisher Scientific, Loughborough, UK), the control also included the corresponding amount of the solvent. After additional 4 h, cells were treated with a half-logarithmic dilution series of either cisplatin ($10^{-3.5}$ to $10^{-7.5}$ M), niraparib ($10^{-3.5}$ to $10^{-7.5}$ M), olaparib (10^{-4} to 10^{-8} M) and incubated for 72 h. Following the incubation period, the assay was performed as described [18]. Normalized sigmoidal dose response curves with variable hill slopes were generated and LC_{50} values were determined by non-linear regression using a four-parameter logistic equation using GraphPad Prism 8 (GraphPad Software, San Diego, CA, USA).

2.7 Western blot

Cell lysis was performed using cell extraction buffer (Bender MedSystems GmbH, Vienna, Austria) supplemented with 10 µl/ml Halt™ protease inhibitor cocktail (Thermo Fisher Scientific Inc., Waltham, MA, USA), 3.2 µl/ml PMSF (Sigma-Aldrich GmbH), and 10 µl/ml Halt™ phosphatase inhibitor cocktail (Thermo Fisher Scientific Inc.). Total protein was quantified using the Pierce™ BCA Protein Assay Kit (Thermo Fisher Scientific Inc.). After protein separation by SDS-PAGE with 20 µg protein per lane on stain-free gels (Bio-Rad Laboratories GmbH, Munich, Germany), the further process of Western blotting was carried out as described [18]. We used rabbit anti-pATR (Thr1989) (#30632S), rabbit anti-pATM (Ser1981) (#13050T), rabbit anti-DDR1 (#5583), rabbit anti-p44/42 MAPK (ERK1/2) (Thr202/Tyr204) (D13.14.4E) (#4370), rabbit anti-BRCA1 (Ser1524) (#9009S) (purchased from Cell Signaling Technology, Frankfurt, Germany); mouse anti-PARP1 (#sc-8007), mouse anti-ATM (#sc-377293), mouse anti-RAD51 (#sc-53428), mouse anti-ATR (#sc-515173), mouse anti-BRCA1 (#sc-6954), mouse anti-SLFN11 (#sc-374339), mouse anti-integrin β1 (#sc-59829), rabbit anti-ERK1 (#sc-94) and rabbit anti-ERK2 (#sc-154)

(purchased from Santa Cruz Biotechnology, Heidelberg, Germany); all diluted in TBS-T containing 1 % BA and 0.05 % sdium azide. To visualize the proteins of interest, a Clarity Western ECL substrate chemiluminescence kit (Bio-Rad Laboratories) and ChemiDoc XRS+ imaging acquisition system (Bio-Rad Laboratories) were used. Band intensities were normalized to total protein expression using ImageLab software v 6.0 (Bio-Rad Laboratories) for quantification and analysis.

2.8 Cell cycle analysis

Cells were transferred in 12-well plates (Sarstedt AG) with and without COL1 coating at a density of 300,000 cells and cultivated at 37°C and 5% CO_2 until the next day. Subsequently, cells were treated with 1 µM niraparib or with PBS as control. For combined treatments, 10 nM of the ATRi elimusertib or 1 µM of the ATMi AZD1390 were used combined with niraparib. After an incubation period of 24 h, the assay was performed as described [23]. To analyze the cell cycle, a Guava® easyCyte HT 11 Flow Cytometer (Luminex Corporation, Austin, TX, USA) and FlowJo™ v10.5.3 Software (BD Life Sciences, Franklin Lakes, NJ, USA) were used.

2.9 Annexin V-FITC/PI apoptosis assay

Apoptosis induction was analyzed using an Annexin V-FITC/PI assay. 80,000 cells were seeded per well in 12-well plates (Sarstedt AG) coated with COL1 or left uncoated and treated after 24 h with either PBS as control, 5 µM niraparib, or in combination with 10 nM ATRi elimusertib, or 1 µM ATMi AZD1390, or 1 µM ERKi SCH772984. After a 72 h incubation period, cells were collected, washed with a staining buffer (HEPES 0.1 M, NaCl 1.4 M, $CaCl_2 \times 3\ H_2O$ 25 mM), resuspended in 450 µl of the same buffer containing 0.2 µl/well Annexin V FITC (BioLegend, San Diego, CA, USA) and 0.5 µl/well propidium iodide (Life Technologies Corporation) and transferred in triplicates to a 96 well plate (ThermoFisher Scientific, Rochester, NY, USA). After 15 minutes of incubation, the samples were analyzed by flow cytometry using Guava® esayCyteTM (Luminex Corporation). Compensation and determination of apoptosis ratio were performed via FlowJo™ v10.5.3 Software (BD biosciences)

2.10 NAD/NADH-Glo™-assay

To evaluate the impact of COL1 binding on total oxidized and reduced nicotinamide adenine dinucleotide (NAD^+ and NADH) levels, a bioluminescent NAD/NADH-Glo™-assay (Promega Corp., Madison, W1, USA) was performed. 384-well white-walled tissue culture plates (Greiner Bio-One GmbH., Frickenhausen, Germany) were partially coated with COL1. W1, W1CR, W1NR, A2780, and A2780cis cells were seeded at a density of 1800 cells per well and incubated for 24 h. Afterwards, the cells were treated with either 1 µM or 10 µM niraparib and incubated for additional 24 h. NAD/NADH-Glo™ detection reagents were prepared according to the manufacturer`s protocol and added to the cells, maintaining a 1:1 volume ratio between sample and detection reagent. After an incubation period of 45 minutes in the dark, luminescence was recorded by Tecan Spark microplate reader (Tecan Trading AG, Männedorf, Switzerland). Background measurement was subtracted, data were normalized to control, and analyzed using GraphPad Software.

2.11 Statistical analysis

The statistical analysis was performed using GraphPad Prism 8 (GraphPad Software). Resistance factors and log2 fold changes are represented as median with 95% CI. All other data are displayed as means ± SD. To test for significant changes through pre-treatment with inhibitors or COL1-binding, we performed paired t-tests, while differences between two different cell lines were analyzed with an unpaired t-test. To check for significance differences between more than two groups, a two-way ANOVA was applied (asterisks indicate *$P < 0.05$; **$P < 0.01$; ***$P < 0.001$; ****$P < 0.0001$, asterisks above columns show significance to the respective control).

3 Results

3.1 Evaluating the role of adhesion molecules in the formation of CAM-CR in ovarian cancer cells

COL1 has recently shown to induce resistance to niraparib and olaparib in W1, W1CR, and A2780cis cells, but not in A2780 cells [18]. Here, we analyzed COL1 adhesion of these cell lines relative to uncoated controls. W1 and W1CR cells displayed increased adhesion to COL1-coated surfaces relative to uncoated surfaces. In contrast, COL1 coating reduced A2780 and A2780cis cell adhesion. Notably, A2780cis cells formed suspension cell aggregates without signs of any adherence on COL1-coated surfaces (Fig. 1a-b). These findings indicate that the investigated cell lines differ in their interactions with COL1 and that CAM-DR may be caused by varying mechanisms.

Next, we tested three additional ovarian cancer cell lines (Kuramochi cells, its cisplatin-resistant subline Kuramochi^{r}CDDP^{2000}, and the intrinsically cisplatin-resistant EFO21 cell line) for their sensitivity to cisplatin and the PARPi olaparib and niraparib in the absence and presence of COL1. COL1 did not affect the sensitivity of EFO21 and Kuramochi'CDDP^{2000} cells to any of the drugs. Kuramochi cells displayed enhanced resistance to olaparib in the presence of COL1, but not to cisplatin or niraparib (Supplement Fig. 1a-b). Subsequently, in an attempt to exploit the role of potential COL1-binding adhesion molecules in the formation of CAM-DR, the cellular expression profiles of integrin β1 (ITGB1) and Discoidin Domain receptor 1 (DDR1) were explored. While DDR1 expression did not differ among the examined cell lines, the CAM-DR-negative A2780, Kuramochi^{r}CDDP^{2000} and EFO21 cells expressed significantly more ITGB1 than the respective cell lines known to form CAM-DR (Fig. 1c-d, Supplement Fig. 1c). Plotting the expression of ITGB1 or DDR1 alongside the COL1-mediated resistance factors across all investigated cell lines revealed a weak, negative correlation between ITGB1 expression and the intensity of CAM-DR (Supplement Fig. 1d).

Mechanistically, there was no consistent correlation between the cellular levels of the COL1-binding adhesion molecules ITGB1 and DDR1 (Fig. 1c-d, Supplement Fig. 1c). In agreement, ITGB1 depletion (Supplement Fig. 2b) and DDR1 inhibition experiments did not suggest a significant role of either protein

in COL1-mediated resistance in W1 and W1CR cells (Fig. 1e-f), raw data of Fig. 1e shown in Supplement Fig. 2a).

To further evaluate the interaction of W1, W1CR, and A2780 cells with a COL1 matrix, these cells were studied by FTIR imaging in order to get more insight into cell surface signature. This analysis displayed changes in the surface composition of all three cell lines when grown on COL1, particularly carbohydrate-related alterations accompanied by secondary protein/lipid contributions (Fig. 1g-i). Moreover, changes in the peaks associated with phosphate-containing functional groups, such as nucleic acids indicate conformational changes of DNA in COL1-cultivated cells. The most remarkable changes were detected as peaks indicating DNA methylation on cytosines in COL1-cultivated cells. A detailed analysis of FTIR spectra is provided in the Supplementary information (Supplement Figs. 3 and 4).

3.2 Acquired niraparib-resistant ovarian cancer cells are not affected by COL1

The impact of COL1 matrices on ovarian cancer cell sensitivity to PARPi had previously been investigated only in cell lines naïve to PARPi treatment. Hence, to determine the relevance of CAM-DR for ovarian cancer at an advanced stage of PARPi therapy, we established a niraparib-resistant subline of the W1 cell line by pulsed exposure to niraparib, referred as W1NR (Fig. 2a). W1NR cells displayed a strongly reduced sensitivity to both PARPi and cross-resistance to cisplatin (Fig. 2b). COL1 decreased the sensitivity of W1 and W1CR to PARPi, and cisplatin. In contrast, COL1 decreased the sensitivity of W1NR to cisplatin, but not to the PARPi olaparib and niraparib (Fig. 2c, raw data are shown in Supplement Fig. 3a).

Reduced cellular levels of PARP1 as the main PARPi target and of the pro-apoptotic helicase SLFN11 have been associated with resistance to PARPi [18, 23]. Indeed, W1NR cells displayed reduced PARP1 levels in relation to W1 and W1CR cells (Fig. 2d), but not affected by COL1 (Supplement Fig. 5b). In contrast to W1CR cells, W1NR cells did not display downregulated SLFN11 levels (Fig. 2e), which were not affected by COL1 and also not by niraparib (Supplement Fig. 5c).

For further investigating the mechanisms underlying COL1-mediated CAM-DR and drug-induced acquired resistance, we used niraparib as it exhibited a higher potency than olaparib in our models.

As the activity of the PARP enzymes, the intensity of PARP trapping, and cell death induction also depends on intracellular NAD^+, we quantified its levels in the different cell lines [10, 24]. However, no differences were detected among the untreated W1 cell lines including W1NR cells. Compared to W1 cells, A2780 and A2780cis cells displayed intrinsically decreased NAD^+ levels (Fig. 2f). COL1 did not affect the cellular NAD^+/NADH ratios in W1, W1CR, W1NR, or A2780 cells in the absence or presence of 1 μM or 10 μM niraparib. Only in A2780cis, COL1 reduced the cellular NAD^+/NADH ratio in the presence of 10 μM niraparib (Fig. 2g, raw data are shown in Supplement Fig. 6). Since PARP-enzyme related data

did not lead to an explanation for the CAM-DR phenomena, we focused on DNA-repair pathways in the following experiments.

3.3 COL1 binding induces heterogeneous changes in the DNA damage response among ovarian cancer cell lines

As mentioned before, the restoration and upregulation of HR is a common resistance mechanism in PARPi therapy. HR is tightly linked to the cell cycle distribution, since its initiation is restricted to the S and early G2-phase [25]. Therefore, we analyzed cell cycle distribution as an integral element of the DNA damage response [26].

Thus, we investigated the impact of COL1 and 1 µM niraparib, a sub-toxic concentration, on the cell cycle distribution in the investigated cell lines. COL1 did not affect the cell cycle on its own. While niraparib treatment resulted in an enhanced proportion of W1 cells in the S-phase distribution, but not of W1CR cells, the combination of niraparib and COL1 induced a massive S-phase shift in W1CR cells, which is more pronounced than the niraparib-mediated cell cycle arrest in W1 cells. In contrast, neither COL1 nor niraparib treatment significantly affected the cell cycle of W1NR cells. A2780 and A2780cis cells displayed a similar behavior (Fig. 3a-e).

The kinases ATR and ATM are key regulators of the DNA damage response, mediating cell cycle arrest and DSB repair via HR afterwards [27]. Consequently, the ATR inhibitor elimusertib and the ATM inhibitor AZD1390 are able to sensitize W1 and W1CR cells to cisplatin and PARPi [18, 23, 26]. Inhibition of both, ATR and ATM, also sensitized W1NR cells to niraparib as well as olaparib (Fig. 2f-g, Supplement Fig. 5d). Interestingly, COL1 antagonized the elimusertib- and AZD1390-mediated effects, although it did not increase the resistance of W1NR cells to PARPi in the single treatment approaches (Fig. 2f-g).

To further elucidate whether the increase in S-phase W1CR cells on COL1 is mediated by ATR or ATM, thus leading to increased DNA repair capacity, concomitant treatments of niraparib with sub-toxic concentrations of either ATRi elimusertib or ATMi AZD1390 were analyzed.

Combined targeting of PARP and ATR/ATM shifted W1 and W1CR cells to the G2-phase, thereby preventing S-phase accumulation. This effect was especially pronounced upon treatment of W1CR cells with the ATMi (Fig. 3h-i). In contrast, the cell cycle of niraparib-resistant W1NR cells was neither affected by niraparib treatment nor by contact with COL1, demonstrating a high stability in cell cycle regulation. Remarkably, targeting ATR and ATM in combination with niraparib also did not induce a phase shift, which is a striking difference from the other W1 cells (Fig. 3j).

3.4 A further insight into COL1-mediated DNA repair capacity

We further focused on the capacity of homologous recombination (HR) repair in the respective cell lines as it is the most important pathway for the repair of PARPi induced DNA damages [14]. Furthermore, this pathway only occurs during S- and G2-phase of the cell cycle which checkpoints are triggered by the previously investigated treatments [25].

Western blot data confirm that key players involved in HR (BRCA1, ATR, ATM, RAD51) displayed similar abundance and phosphorylation levels in W1 and W1CR cells (Fig. 4a, raw data are exhibited in Supplement Fig. 7). In contrast, W1NR cells displayed elevated ATM phosphorylation and reduced BRCA1 and RAD51 levels. A2780cis cells were generally characterized by higher abundance and phosphorylation levels of homologous recombination proteins, which was most notable for BRCA1 and ATR (Fig. 4a, raw data are exhibited in Supplement Fig. 7).

In relation to that we investigated the role of HR proteins in COL1-mediated PARPi resistance. For this purpose, niraparib was used at low (1 µM) and high (10 µM) concentrations, whereas due to the high sensitivity, W1 cells were only treated with 1 µM niraparib. Western blot data revealed that treatment with niraparib increased the levels of all activated regulators in the indicated cell lines (Fig. 4b; raw data are shown in Supplement Figs. 7 and 8), further reflected by illustrating the protein ratios of phosphorylated versus non-phosphorylated species (Fig. 4c-e, Supplement Fig. 8). This effect was more pronounced at the higher niraparib concentration.

COL1 significantly increased RAD51 expression in niraparib-treated W1 and A2780cis cells. To a lesser extent, this effect was observed in W1CR and W1NR cells, but not in A2780 cells (Supplement Fig. 9). Aside from that, the response of A2780 cells was similar to that of W1 cells. COL1 binding also affected BRCA1 activation in W1 cells. As previously reported, contact with COL1 enhanced the niraparib-mediated activation of ATR in W1 and W1CR cells, whereas ATM activation was not further increased [18].

Without COL1, W1NR cells exhibited a similar expression profile to W1CR cells despite a stronger activation of ATM at high niraparib concentrations. However, their response profile differed upon COL1. In contrast to W1 and W1CR cells, W1NR cells express elevated levels of activated ATM at lower niraparib concentrations. Furthermore, W1NR displayed a more pronounced COL1-mediated upregulation of total BRCA1 expression and activation. Interestingly, at higher niraparib concentration, COL1 attenuated the activation of ATR in W1CR and of ATR and ATM in W1NR cells induced by niraparib treatment (Fig. 4b, raw data are shown in Supplement Fig. 7, Supplement Fig. 8).

Taken together, it became evident that W1NR cells have the highest potential to activate HR-related proteins in the absence of COL1. Surprisingly, the protein expressions were not further enhanced by COL1 in both resistant cell lines W1CR and W1NR. This leads to the conclusion that other pathways than DNA repair must be involved in COL1-mediated resistance against PARPi and combinational treatments with ATRi and ATMi.

3.5 Analysis of the underlying signaling pathways reveals targets for sensitization

Since targeting DNA repair mechanisms failed to overcome the acquired PARPi resistance of W1NR cells, and the underlying signaling following COL1 binding remains unclear, an inhibitor screening of classical COL1-associated proteins was performed to identify sensitization targets for acquired PARPi resistance. We selected a panel of inhibitors of distinct signaling molecules (JNK1/2/3 (tanzisertib), p38 MAPK (adezmapimod), ERK1/2 (SCH772984), ALK/c-Met (crizotinib), pan-PI3K/m-TOR (dactolisib), WNT (pyrivinium), FAK (FAK-IN-14) known to be potentially associated with PARPi resistance or CAM-DR [17, 28–32]. Their impact on cell vitality was tested on their own and in combination with the PARPi niraparib and olaparib in the absence or presence of COL1 in W1, W1CR, and W1NR cells, resulting in complex drug response patterns (Fig. 5a or c and Fig. 5b or d, respectively; raw data are displayed in Supplement Fig. 10–11).

Among the examined targets, inhibition of WNT resulted in a pronounced increase in olaparib effectiveness in W1, W1CR and W1NR cells, regardless of cultivation on COL1 (Fig. 5c-e). In contrast, WNT inhibition did not affect niraparib activity (Fig. 5a, b, e). Potential targets to overcome CAM-DR against niraparib in W1 and W1CR cells include JNK signaling and the co-inhibition of PI3K/m-TOR. Notably, these inhibitors were only effective in niraparib-treated W1 cells with contact with COL1. Furthermore, the dual PI3K/m-TOR inhibitor elicited a reverse effect in concomitant treatment with olaparib.

The response of the acquired niraparib-resistant W1NR to the indicated inhibitors differed from that of the other examined cell lines (Fig. 5e). Only the ERK inhibitor consistently increased the efficacy of both, niraparib and olaparib in this cell line. Notably, single ERK inhibitor treatment also already reduced cell viability (Supplement Fig. 12a). Hence, ERK inhibition may have potential for sensitizing acquired PARPi resistant cancer cells.

3.6 ERK is a promising target to overcome acquired PARPi resistance

To further evaluate the role of ERK signaling in COL1-mediated and acquired PARPi resistance, its expression and activation in niraparib-treated W1, W1CR and W1NR cells was analyzed. To tackle the mechanism of the previously demonstrated insufficient sensitization of W1NR cells to PARPi by ATR/ATM inhibition (Fig. 3), the potential involvement of this pro-survival pathway (Fig. 3) was further exploited. Neither niraparib treatment nor COL1 cultivation altered the abundance or phosphorylation of ERK1/2 in W1, W1CR, and W1NR cells. However, combined treatment of niraparib with ATRi or ATMi resulted in enhanced ERK1/2 phosphorylation in W1NR cells (Fig. 6a-c, Supplement Fig. 12b).

Consequently, we analyzed whether the combination of ERKi (1 μM) with ATRi (10 nM), or with ATMi (1 μM) increases the efficiency of PARPi treatment in W1NR cells, reflected by the Annexin/PI apoptosis

assay when using niraparib at 5 μM (Fig. 6d). The results display a significant reduction in cell viability compared to solely treatment with the ERKi, further enhanced by the combination with niraparib. In contrast, treatment with a triple combination of niraparib, ERKi, and either ATRi or ATMi exhibited no additional sensitization beyond the aforementioned dual combination. In contrast, evaluation of this triple combination via MTT cell viability assay displayed a decreased IC_{50} of niraparib compared to the respective dual combination. Combined niraparib and ERKi treatment was also effective in COL1-cultivated W1NR cells, albeit the sensitization was slightly decreased, as schematically depicted in Fig. 6f.

4 Discussion

Resistance formation to PARPi remains a major obstacle in ovarian cancer treatment. Although it has been demonstrated that CAM-DR is an important factor in the development of PARPi resistance, the underlying mechanisms and its relevance in advanced-stage tumors remain to be elucidated.

Our data show CAM-DR is mediated in ovarian cancer cells by complex mechanisms that do not necessarily depend on known adhesion molecules, such as DDR1 and ITGB1, and differ between drugs, such as cisplatin and PARPi [33]. FTIR analysis suggested that alterations in the carbohydrate composition (dominated by C-O, C-O-C, and glycosidic vibrations) due to COL1 binding may contribute to CAM-DR. In addition, COL1-induced DNA methylation may be involved in mediating drug resistance.

While COL1 reduced PARPi sensitivity of parental ovarian cancer cell lines and their cisplatin-resistant sublines, COL1 did not have an impact on the sensitivity of the niraparib-resistant W1 subline W1NR to niraparib and olaparib. In agreement, W1NR and the cisplatin-resistant W1 subline W1CR displayed distinct expression profiles of PARP1 and SLFN11.

In contrast to W1 and W1CR cells, which had previously been shown to be sensitized to PARPi by ATR and ATM inhibition [18], ATR and ATM inhibitors had a smaller impact on the PARPi sensitivity of W1NR. COL1 further counteracted the actions of ATR and ATM inhibitors, indicating that it promotes survival in advanced-stage ovarian cancer cells in response to DNA damage.

W1, W1CR, and W1NR cells also differed in the regulation of the HR pathway, which can be activated by ATR and ATM. In W1 and W1CR cells, ATR/RAD51 signaling was activated by COL1, while the level of phosphorylated ATM increased in W1NR cells in response to COL1.

The use of a panel of inhibitors against several MAPK and associated proteins revealed complex roles of the respective proteins in COL1-mediated PARPi resistance. WNT inhibition sensitized W1 and W1CR cells to olaparib. JNK and PI3K/mTOR inhibition sensitized them to niraparib.

W1NR cells were highly sensitive to ERK inhibition alone and in combination with PARPi. Furthermore, W1NR cells displayed upregulated ERK signaling in response to ATM and ATR inhibition. Inhibition of ERK could also reverse COL1-mediated ATMi resistance in combination with either niraparib or olaparib.

Taken together, the mechanisms underlying CAM-DR in ovarian cancer cells are complex and differed between different drugs and cell lines, in particular between PARPi-sensitive parental cells and their PARPi-resistant subline. Although, COL1 did not affect the PARPi sensitivity of niraparib-resistant W1NR cells, COL1 had still an effect on DNA repair in this cell line. Finally, we identified ERK inhibition as a promising way to sensitize PARPi-resistant cells to PARPi. A better understanding of these complex processes will be required for the rational design of improved therapies for ovarian cancer.

Declarations

Ethics approval

Not applicable.

Consent for publication

All authors have agreed to publish this manuscript.

Competing Interests

The authors declare no competing interests.

Funding

This study has been supported by German Research Foundation (DFG) in terms of GRK 2873 *'Tools and Drugs of the Future'*.

Author Contribution

LB, PK and GB designed this study. LB, LK & HS performed experiments and analyzed the data. VU acquired the FTIR data and performed the chemometric analysis. SB and GDS conducted the spectral interpretation. GB supervised this project. LB, PK, SB, GDS, JC, MM & GB wrote the manuscript.

Acknowledgement

The authors would like to thank Radoslaw Januchowski, Univ. of Zielona Gora, Poland for providing W1 and W1CR cells. Additionally, we are grateful for Florian Rothweiler who organized shipping of Kuramochi, KuramochirCDDP2000 and EFO21 cells. We are very grateful for Svenja Henze who performed Western blot experiments. The collaboration with S.B. and G.D.S., Université de Reims were

embedded into the EU Marie Skłodowska-Curie Actions (MSCA) projects #101086322 HEPINIB. Finally, the authors equally thank the URCATech IBiSA PICT platform for the FTIR imaging facilities.

Data Availability

All data supporting the findings of this study are available within the paper and its Supplementary Information.

References

1. F. Bray, M. Laversanne, H. Sung, J. Ferlay, R.L. Siegel, I. Soerjomataram, A. Jemal, CA: a cancer journal for clinicians (2024) doi:10.3322/caac.21834
2. G. Caruso, S.J. Weroha, W. Cliby, JAMA (2025) doi:10.1001/jama.2025.9495
3. A. González-Martín, P. Harter, A. Leary, D. Lorusso, R.E. Miller, B. Pothuri, I. Ray-Coquard, D.S.P. Tan, E. Bellet, A. Oaknin, J.A. Ledermann, Annals of oncology : official journal of the European Society for Medical Oncology (2023) doi:10.1016/j.annonc.2023.07.011
4. L. Kuroki, S.R. Guntupalli, BMJ (2020) doi:10.1136/bmj.m3773
5. G. Caruso, F. Tomao, G. Parma, M. Lapresa, F. Multinu, I. Palaia, G. Aletti, N. Colombo, International journal of gynecological cancer : official journal of the International Gynecological Cancer Society (2023) doi:10.1136/ijgc-2022-004149
6. I.L. Ray-Coquard, A. Leary, S. Pignata, C. Cropet, A.G. Martin, G. Bogner, H. Yoshida, I.B. Vergote, N. Colombo, J. Maenpaa, F. Selle, B. Schmalfeldt, G. Scambia, E.G. Alia, C. Lefeuvre-Plesse, A. Belau, A. Lortholary, M. Gropp-Meier, E. Pujade-Lauraine, P. Harter, Annals of Oncology (2022) doi:10.1016/j.annonc.2022.08.025
7. J.-C. Amé, C. Spenlehauer, G. de Murcia, BioEssays : news and reviews in molecular, cellular and developmental biology (2004) doi:10.1002/bies.20085
8. J. Ménissier de Murcia, M. Ricoul, L. Tartier, C. Niedergang, A. Huber, F. Dantzer, V. Schreiber, J.-C. Amé, A. Dierich, M. LeMeur, L. Sabatier, P. Chambon, G. de Murcia, The EMBO journal (2003) doi:10.1093/emboj/cdg206
9. T. Helleday, Molecular oncology (2011) doi:10.1016/j.molonc.2011.07.001
10. A.A. Gopal, B. Fernandez, J. Delano, R. Weissleder, J.M. Dubach, Cell Chemical Biology (2024) doi:10.1016/j.chembiol.2023.12.019
11. A. Thomas, J. Murai, Y. Pommier, The Journal of clinical investigation (2018) doi:10.1172/JCI120388
12. R. Purwar, R. Ranjan, M. Pal, S.K. Upadhyay, T. Kumar, M. Pandey, World Journal of Surgical Oncology (2023) doi:10.1186/s12957-023-03027-4
13. X. Jiang, X. Li, W. Li, H. Bai, Z. Zhang, Journal of cellular and molecular medicine (2019) doi:10.1111/jcmm.14133

14. P.-B. Kanev, A. Atemin, S. Stoynov, R. Aleksandrov, Seminars in Oncology (2024) doi:10.1053/j.seminoncol.2023.08.001
15. X. Fu, P. Li, Q. Zhou, R. He, G. Wang, S. Zhu, A. Bagheri, G. Kupfer, H. Pei, J. Li, Genes & diseases (2024) doi:10.1016/j.gendis.2023.02.014
16. S. Kulkarni, N. Seneviratne, Ç. Tosun, S. Madhusudan, DNA Repair (2025) doi:10.1016/j.dnarep.2025.103830
17. Y. Huang, Y. Wang, J. Tang, S. Qin, X. Shen, S. He, S. Ju, Frontiers in cell and developmental biology (2021) doi:10.3389/fcell.2021.698047
18. P. König, L. Bade, J.M. Eichhorn, H. Skalski, J. Cinatl, M. Michaelis, G. Bendas, Cell death discovery (2025) doi:10.1038/s41420-025-02740-1
19. K. Wantoch von Rekowski, P. König, S. Henze, M. Schlesinger, P. Zawierucha, R. Januchowski, G. Bendas, Biomolecules (2019) doi:10.3390/biom9120788
20. R. Januchowski, P. Zawierucha, M. Andrzejewska, M. Ruciński, M. Zabel, Biomedicine & pharmacotherapy = Biomedecine & pharmacotherapie (2013) doi:10.1016/j.biopha.2012.11.011
21. Industrial Biotechnology Centre, The Resistant Cancer Cell Line (RCCL) collection - Industrial Biotechnology Centre - Research at Kent (2023), https://research.kent.ac.uk/industrial-biotechnology-centre/the-resistant-cancer-cell-line-rccl-collection/. Accessed 8 January 2025
22. H.T. Mohamed, V. Untereiner, G. Cinque, S.A. Ibrahim, M. Götte, N.Q. Nguyen, R. Rivet, G.D. Sockalingum, S. Brézillon, Molecules (2020) doi:10.3390/molecules25184300
23. P. König, J.M. Eichhorn, E. Suparman, N. Bückreiß, J. Cinatl, M. Michaelis, G. Bendas, Biochimica et Biophysica Acta (BBA) - Molecular Basis of Disease (2024) doi:10.1016/j.bbadis.2024.167448
24. M.M. Murata, X. Kong, E. Moncada, Y. Chen, H. Imamura, P. Wang, M.W. Berns, K. Yokomori, M.A. Digman, Molecular biology of the cell (2019) doi:10.1091/mbc.E18-10-0650
25. W. Zhao, C. Wiese, Y. Kwon, R. Hromas, P. Sung, Annual review of biochemistry (2019) doi:10.1146/annurev-biochem-013118-111058
26. Y. Drew, F.T. Zenke, N.J. Curtin, Nat Rev Drug Discov (2025) doi:10.1038/s41573-024-01060-w
27. J. Smith, L.M. Tho, N. Xu, D.A. Gillespie, Advances in cancer research (2010) doi:10.1016/B978-0-12-380888-2.00003-0
28. Y. Du, H. Yamaguchi, Y. Wei, J.L. Hsu, H.-L. Wang, Y.-H. Hsu, W.-C. Lin, W.-H. Yu, P.G. Leonard, G.R. Lee, M.-K. Chen, K. Nakai, M.-C. Hsu, C.-T. Chen, Y. Sun, Y. Wu, W.-C. Chang, W.-C. Huang, C.-L. Liu, Y.-C. Chang, C.-H. Chen, M. Park, P. Jones, G.N. Hortobagyi, M.-C. Hung, Nat Med (2016) doi:10.1038/nm.4032
29. S.E. Golding, E. Rosenberg, S. Neill, P. Dent, L.F. Povirk, K. Valerie, Cancer Res (2007) doi:10.1158/0008-5472.CAN-06-2371
30. T.M. Yamamoto, A. McMellen, Z.L. Watson, J. Aguilera, R. Ferguson, E. Nurmemmedov, T. Thakar, G.-L. Moldovan, H. Kim, D.M. Cittelly, A.M. Joglar, E.P. Brennecke, H. Wilson, K. Behbakht, M.J. Sikora, B.G. Bitler, Molecular carcinogenesis (2019) doi:10.1002/mc.23064

31. V. Picco, G. Pagès, Genes & Cancer (2013) doi:10.1177/1947601913486347
32. D. Wang, M. Wang, N. Jiang, Y. Zhang, X. Bian, X. Wang, T.M. Roberts, J.J. Zhao, P. Liu, H. Cheng, Oncotarget (2016) doi:10.18632/oncotarget.7549
33. K. Wantoch von Rekowski, P. König, S. Henze, M. Schlesinger, P. Zawierucha, R. Januchowski, G. Bendas, International journal of molecular sciences (2020) doi:10.3390/ijms21239240

Figures

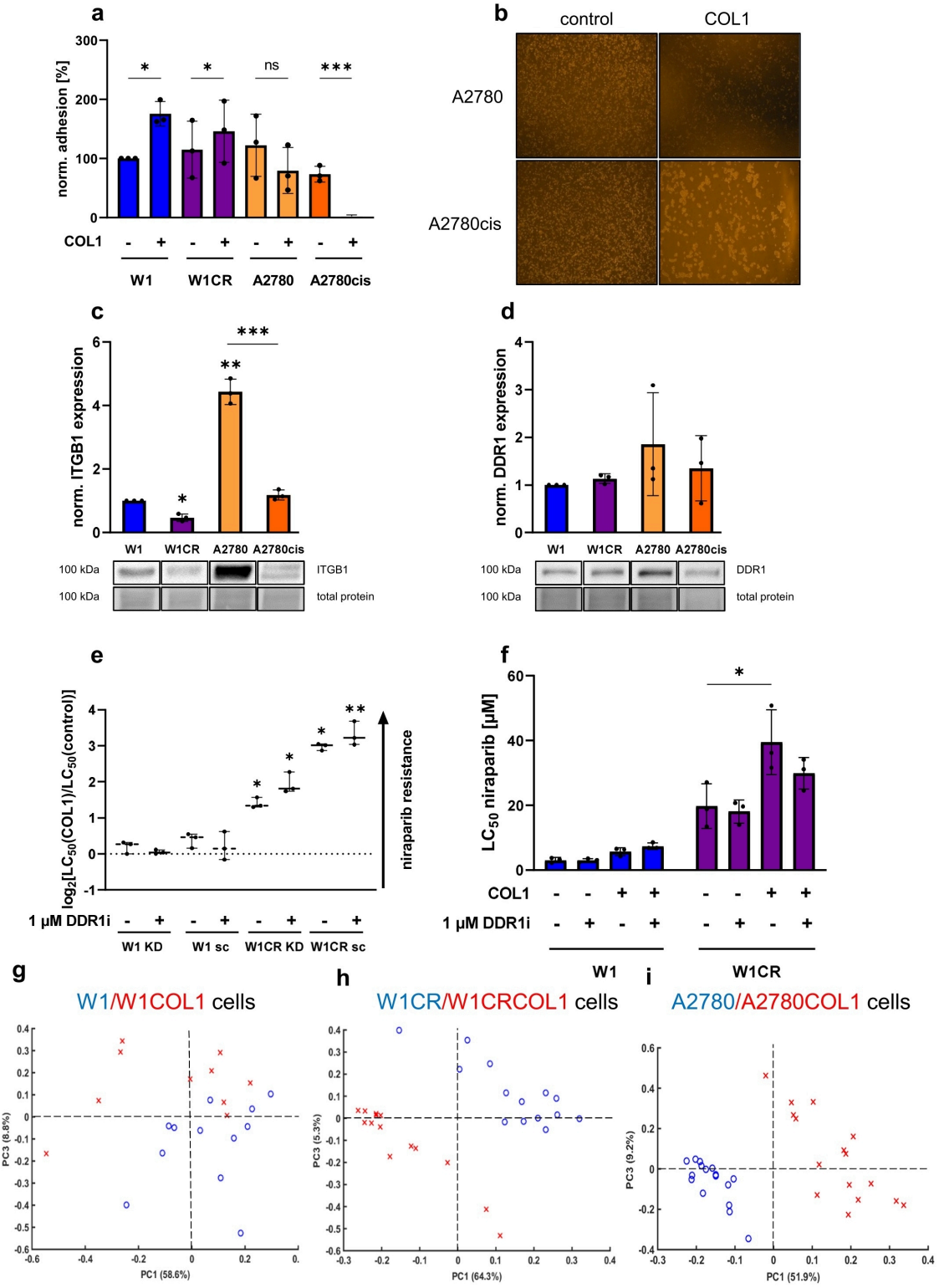


Figure 1

a Relative adhesion of the respective cell lines either on the surface of a plate or on a COL1 matrix normalized to W1 cells on a plate`s surface. Mean ± SD (n = 3), for statistical analysis two-tailed unpaired t-test was performed, *P < 0.05, ***P < 0.001. **b** Microscopic images of morphological characteristics of A2780 and A2780cis cells on plain and COL1-coated plate surface **c-d** Depiction of relative protein expressions of ITGB1 (**c**) and DDR1 (**d**) normalized to W1 cells. Protein bands of

representative Western blots and the respective total protein bands of the stainfree visualization are presented below the histograms. Mean ± SD (n = 3), for statistical analysis two-tailed ratio-paired t-test was performed, *P < 0.05, **P < 0.01; ***P < 0.001. **e** Impact of ITGB1 knockdown on collagen-mediated PARPi resistance. Data is represented as log_2 fold changes between niraparib LC_{50} values of ovarian cancer cells with and without contact with COL1. This is shown for solo or combined (niraparib +DDR1/2 inhibitor) treated W1 and W1CR cells with either an ITGB1 knockdown or a scramble control. Median ± CI (n = 4), to test for significance two-tailed paired t-tests were applied, *P < 0.05, **P < 0.01. **f** Histogram depicts the cytotoxicity of solo (niraparib) and combination (niraparib +DDR1/2 inhibitor) treatment on W1 and W1CR cells cultivated with and without COL1. Mean ± SD (n = 3), for statistical analysis two-tailed paired t-test was used, *P < 0.05. **g-i** PCA analysis of second derivative FTIR spectra of W1 (g), W1CR (h), and A2780 cells (i) cultivated with (red crosses) and without (open blue circles) COL1. PCA was computed on the 900-1400 cm^{-1} spectral range after baseline correction, second derivation and vector normalization of the FTIR spectra. The corresponding loadings are shown in supplementary Figure 3.

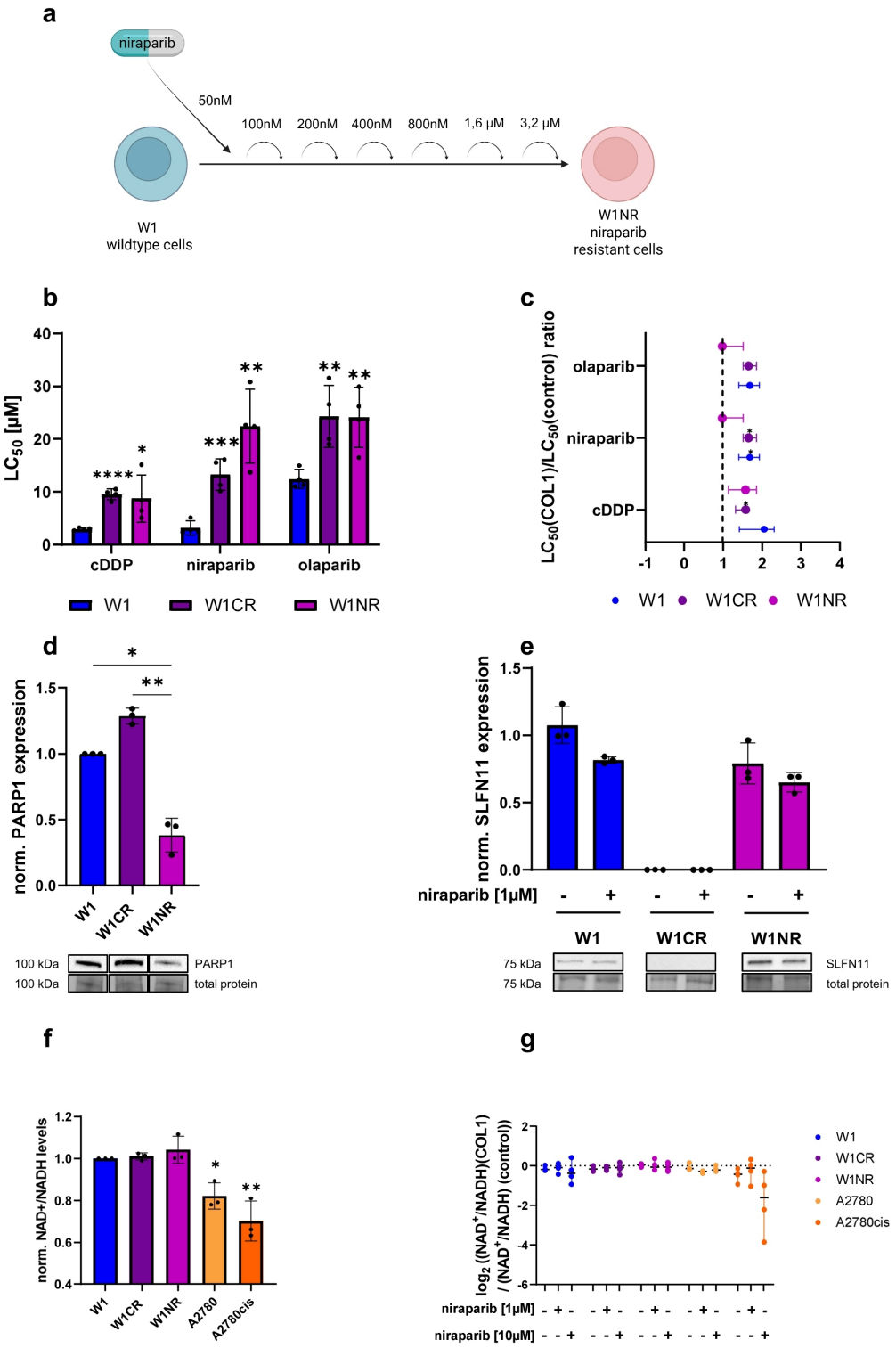


Figure 2

a Graphical representation of the process for establishing the niraparib-resistant subline W1NR. This graphic was created with biorender.com **b** IC50 values of either cisplatin, niraparib and olaparib in the W1, W1CR and W1NR cell lines. Mean ± SD (n = 4), for statistical analysis two-tailed paired t-tests were performed *P < 0.05, **P < 0.01; ***P < 0.001. **c**Ratio of cisplatin, niraparib and olaparib IC50 values between the respective ovarian cancer cells cultivated with and without COL1. This is displayed for W1,

W1CR and W1NR cells. Median ± CI (n = 3), to test for significance two-tailed paired t-tests were applied, *P < 0.05. **d** Representative Western Blot of PARP1 in the W1 cells and their resistant sublines. Histogram depicts relative protein expression of PARP1 normalized on W1 cells. Mean ± SD (n = 3), for statistical analysis two-tailed ratio-paired t-test was performed, *P < 0.05, **P < 0.01. **e** displays the relative expressions of SLFN11 in untreated W1, W1CR and W1NR and the respective cells treated with 1 µM niraparib for 24 hours. Expression was normalized to untreated W1 cells. Mean ± SD (n = 3), for statistical analysis two-tailed ratio-paired t-test was performed. Protein bands of the respective total protein bands of the stainfree visualization of d and e are presented below. **f** displays the relative NAD+/NADH levels in the respective cell lines normalized to untreated W1 cells. Mean ± SD (n = 4), to test for statistical significance two-tailed Welch`s t test was applied. **g** Impact of COL1 binding and treatment with 1 µM niraparib for 24 hours on metabolic and PARP activity in the respective ovarian cancer cells. Data is depicted as log2 fold changes between NAD+/NADH levels of the respective ovarian cancer cells cultivated with and without COL1. (Median ± CI).

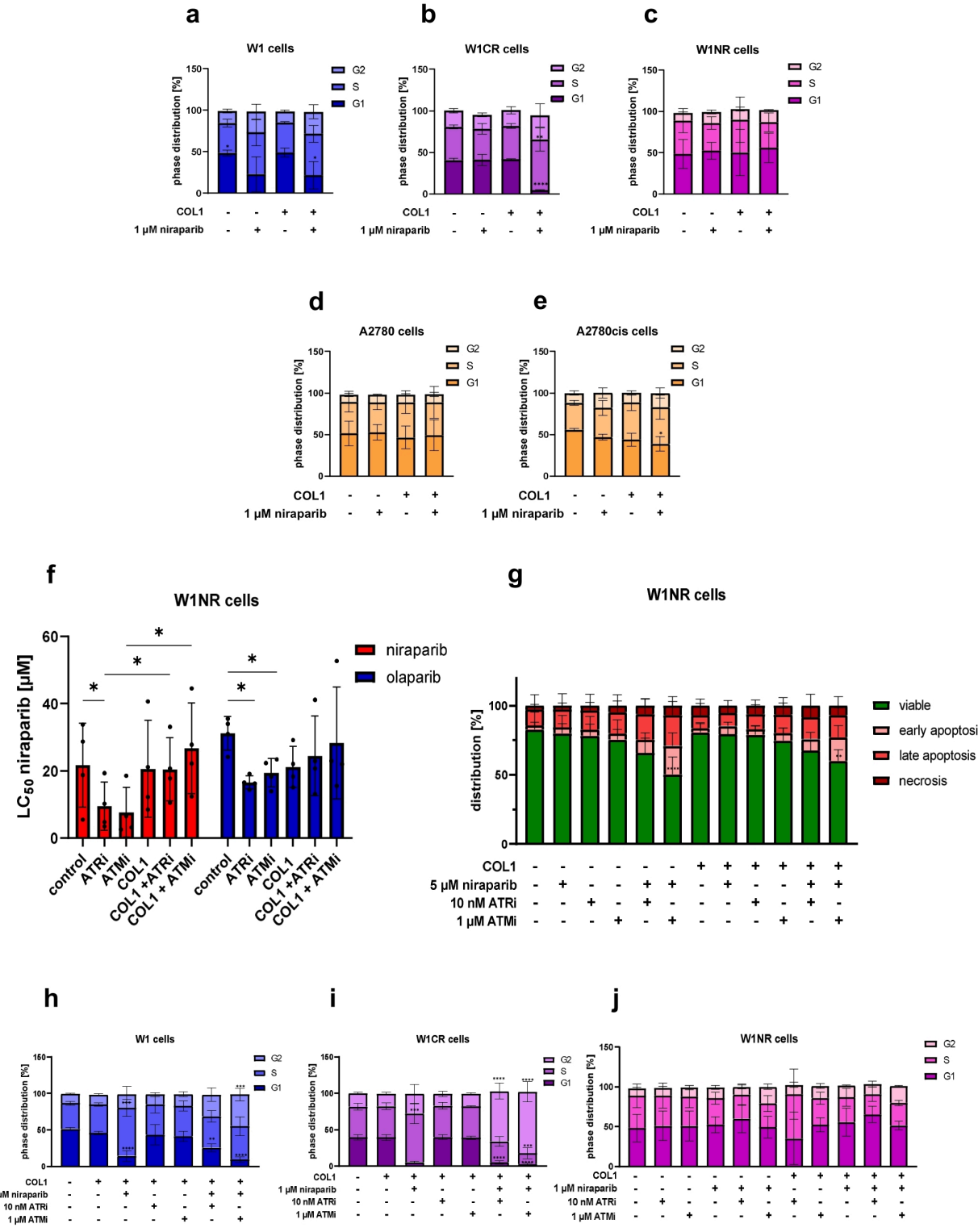


Figure 3

a-e Cell cycle analysis of the indicated cell lines (W1 (**a**), W1CR (**b**), W1NR (**c**), A2780 (**d**), A2780cis (**e**) cultivated with and without COL1. Cells were either treated with 1 µM niraparib for 24 hours or remain untreated. Mean ± SD (n = 3) for the respective cell cycle phase, for statistical analysis a two-way ANOVA with tukey correction was performed, *P < 0.05, **P < 0.01, ****P < 0.0001. **f** Impact of COL1 binding and concomitant ATR/ATM inhibition on the niraparib and olaparib cytotoxicity in W1NR cells. Histogram

depicts LC_{50}-values of niraparib (red) and olaparib (blue) in different combination with COL1, 10 nM elimusertib (ATRi) and 1μM AZD1390 (ATMi). Mean ± SD (n = 4), for statistical analysis two-tailed paired t-tests were performed, *P < 0.05. **g** Annexin/PI apoptosis analysis of W1NR cells cultivated with and without COL1. The respective cells were treated with either 5 μM niraparib, 1 μM ATMi or 10 nM ATRi alone, or in the combination of niraparib with ATM or ATR inhibition for 72 hours. Mean ± SD (n = 4) to test for significance a two-way ANOVA with tukey correction was performed for each stage of apoptosis and treatment. **h-j** display cell cycle analysis of W1 (**h**), W1CR (**i**) and W1NR cells (**j**) treated with 1 μM niraparib alone or in combination with either 10 nM elimusertib (ATRi) or 1 μM AZD1390 (ATMi) for 24 hours. All W1 and W1CR cells with the exception of untreated control cells were cultivated on COL1 matrices, while W1NR cells were cultivated for each treatment with and without COL1. Mean ± SD (n = 3) for each respective phase and cell line, to test for significance a two-way ANOVA with tukey correction was applied; *P < 0.05, **P < 0.01; ***P < 0.001, ****P < 0.0001.

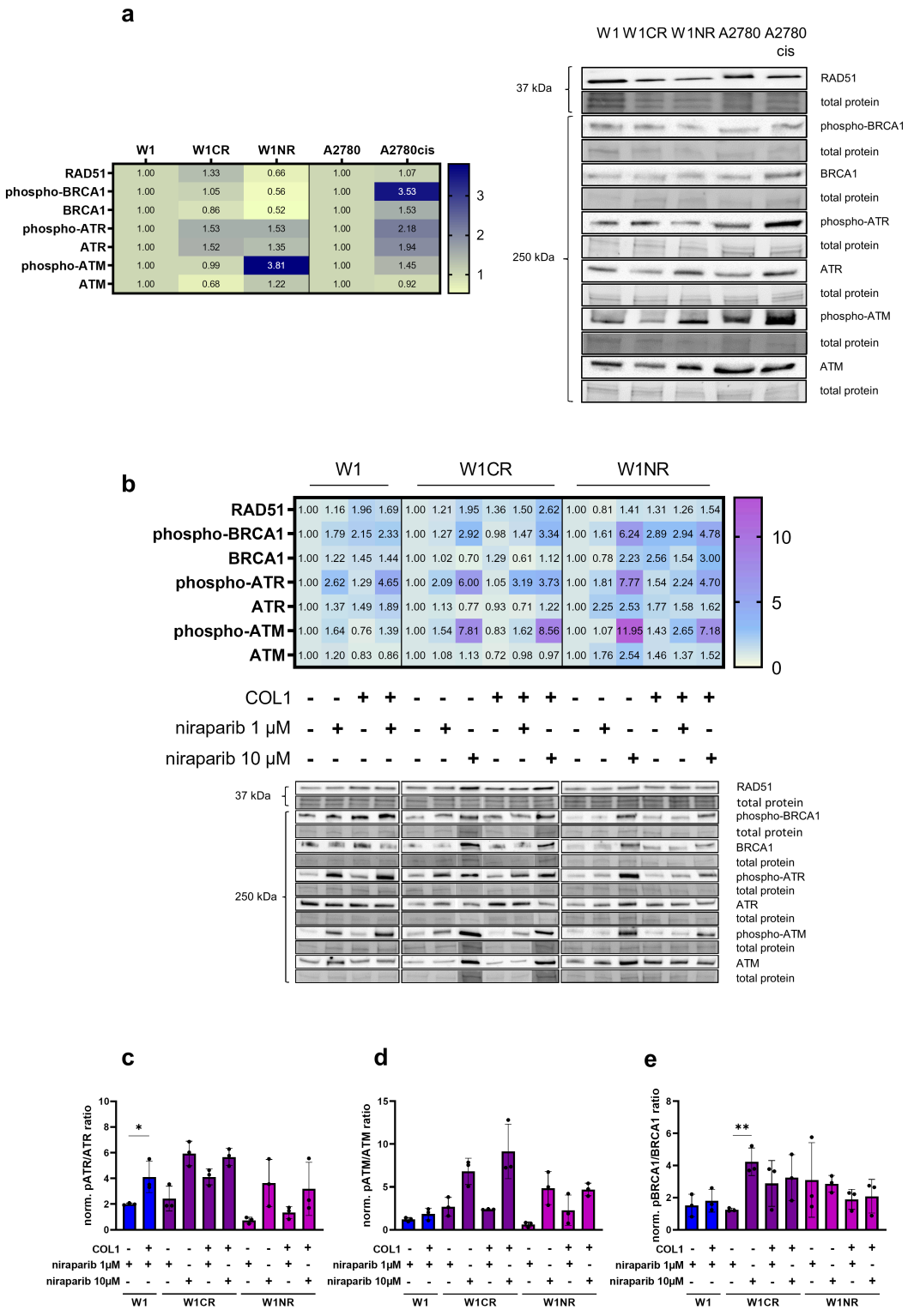


Figure 4

a-b Heatmaps of the expression and activity pattern of various DNA repair proteins in W1 and A2780 cells as well as their resistant sublines. Figure a shows a comparison of relative protein expression among untreated ovarian cancer cells. Data is normalized to the respective sensitive wildtype cell line. Mean (n = 3). Figure b depicts the relative protein expressions of W1 cells and their resistant sublines with either 1 µM or 10 µM niraparib treatment for 24 hours or without treatment. The cells were

cultivated with and without COL1. All expressions are normalized to the untreated control cells without COL1. Mean (n = 3). Representative Western Blot images of the protein bands and the respective total protein band of the stainfree visualization are shown left (a) or below (b). **c-e**Ratio between phosphorylated and un-phosphorylated expression of ATR (**c**), ATM (**d**) and BRCA1 (**e**). This is shown for W1, W1CR and W1NR cells with and without contact with COL1. Cells were treated with 1 µM or 10 µM niraparib for 24 hours. Expression was normalized to their respective untreated control. Mean (n = 3), for significance analysis two-tailed ratio-paired t-tests were performed; *P < 0.05, **P < 0.01.

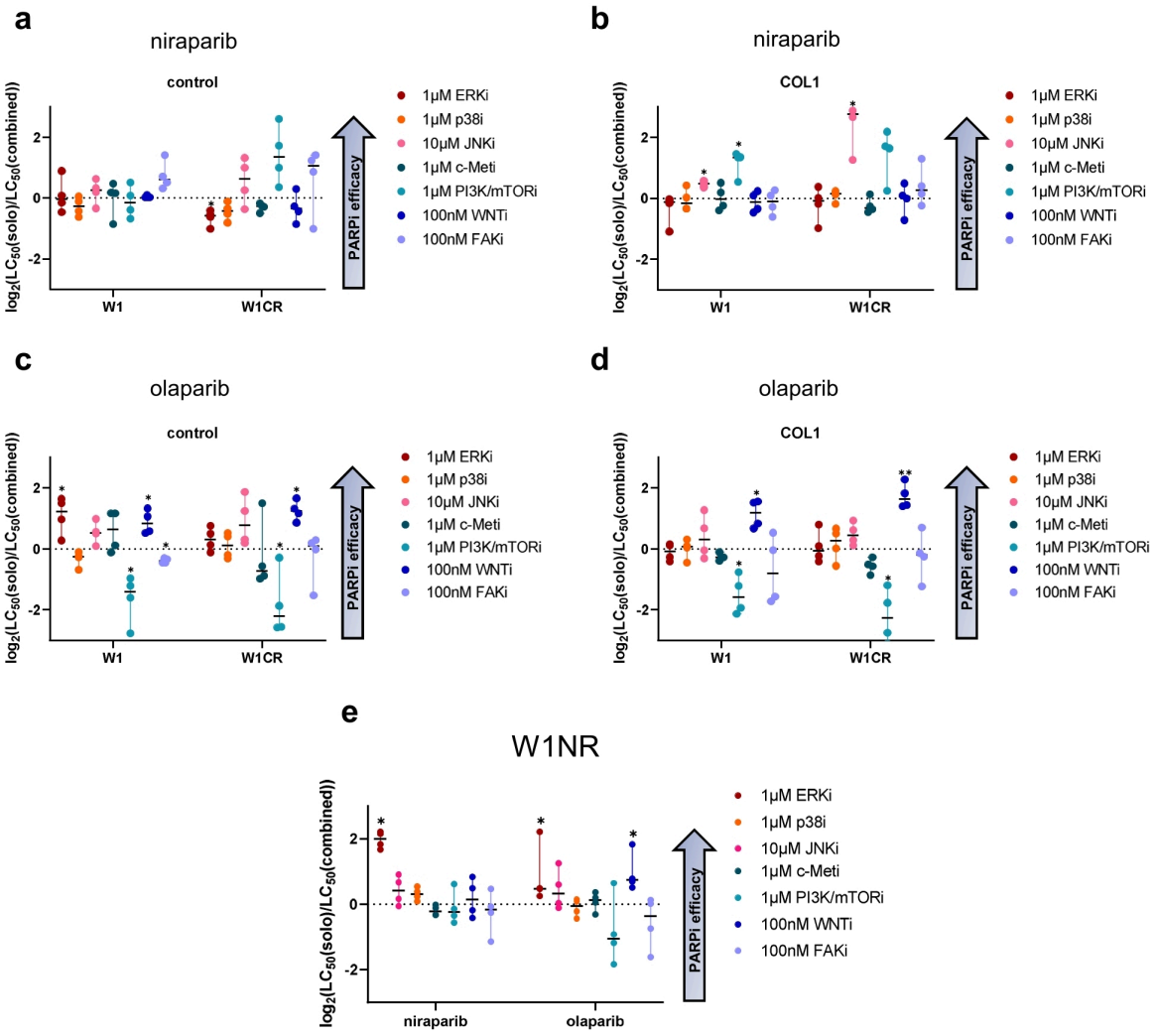


Figure 5

a-e Impact of combinational treatment using a panel of different inhibitors of signaling molecules on the cytotoxicity of niraparib (a, b and e) and olaparib (c, d and e) in W1, W1CR and W1NR cells. Data is displayed as log2 fold changes between LC50-values of solo (PARPi) and combined (PARPi + additional inhibitor) treatment. Cells were either cultivated without (a, c and e) or with COL1 (b and d). Median ± CI (n = 4), to test for significance two-tailed paired t-tests were applied; *P < 0.05, **P < 0.01.

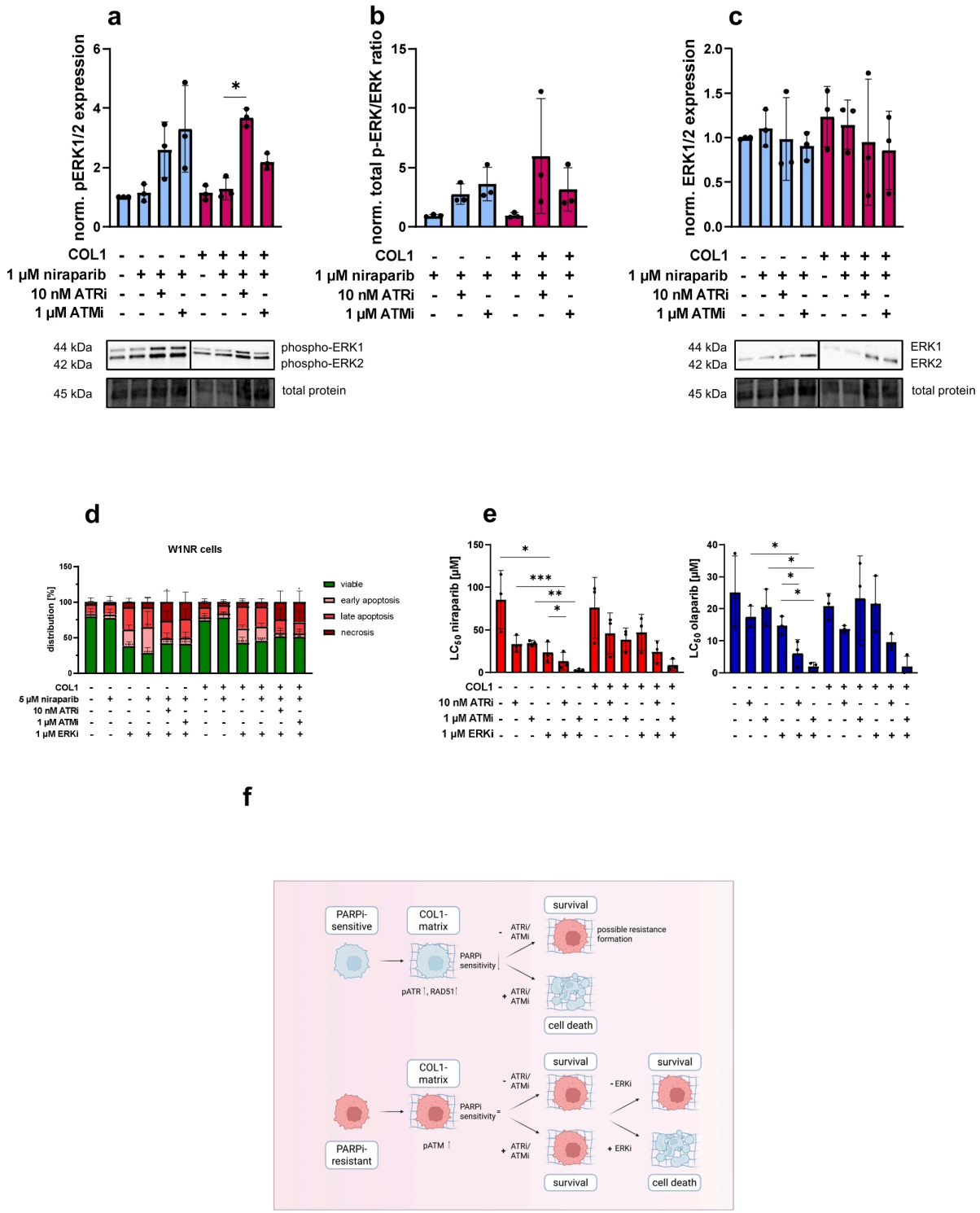


Figure 6

a-b Histograms displays the relative expression of total ERK1/2 in W1NR cells with and without binding COL1 normalized to untreated W1NR cells. Cells were treated with 1 µM niraparib alone or in combination with 10 nM elimusertib (ATRi) or 1 µM AZD1390 (ATMi) for 24 hours. Additionally, untreated cells were analyzed. **a** depicts the expression of phosphorylated ERK1/2, while **c** represents the un-phosphorylated form. Representative Western Blot protein bands and the respective total protein bands of the stainfree visualization are displayed below. Mean ± SD (n = 3), for statistical analysis two-tailed

ratio-paired t-tests were applied; *P < 0.05. **b** Ratio between phosphorylated and un-phosphorylated expression of ERK1/2 shown in a and c in W1NR. Mean ± SD (n = 3), for statistical analysis two-tailed ratio-paired t-tests were applied d Annexin/PI apoptosis analysis of W1NR cells cultivated with and without COL1. The indicated cells were either solo treated with 5 μM niraparib or 1 μM SCH772984 (ERKi), or in double and triple combinations with the aforementioned drugs and additional 10 nM elimusertib (ATRi) or 1 μM AZD1390 (ATMi) for 72 hours. Mean ± SD (n = 4) for statistical analysis a two-way ANOVA with tukey correction was performed for each stage of apoptosis and treatment. **e** Impact of the combined treatment of either the ATRi elimusertib (10 nM) or ATMi AZD1390 (1μM) and the ERKi SCH772984 (1μM) on the nirabarib (red) and olaparib (blue) efficacy in W1NR cells cultivated with and without COL1. Mean ± SD (n = 3), to test for significance two-tailed ratio-paired t-tests were applied; *P < 0.05, **P < 0.01; ***P < 0.001. **f** Graphical representation of the sensitization possibilities of W1 and W1NR cells to PARPi. This illustration was created with biorender.com.

Supplementary Files

This is a list of supplementary files associated with this preprint. Click to download.

- Supplementaryresults.pdf
- SupplementaryFigures.pdf
- Supportinginformationfullblots.pdf